Polymeric cantilever integrated with PDMS/graphene composite strain sensor

Young-Soo Choi, Min-Joo Gwak, and Dong-Weon Lee

Citation: Review of Scientific Instruments **87**, 105004 (2016); doi: 10.1063/1.4962925
View online: http://dx.doi.org/10.1063/1.4962925
View Table of Contents: http://scitation.aip.org/content/aip/journal/rsi/87/10?ver=pdfcov
Published by the AIP Publishing

REVIEW OF SCIENTIFIC INSTRUMENTS **87**, 105004 (2016)

Polymeric cantilever integrated with PDMS/graphene composite strain sensor

Young-Soo Choi,[a] Min-Joo Gwak,[a] and Dong-Weon Lee[b]
MEMS and Nanotechnology Lab, School of Mechanical Engineering Chonnam National University, Gwangju 500757, South Korea

(Received 10 March 2016; accepted 3 September 2016; published online 12 October 2016)

This paper describes the mechanical and electrical characteristics of a polydimethylsiloxane (PDMS) cantilever integrated with a high-sensitivity strain sensor. The strain sensor is fabricated using PDMS and graphene flakes that are uniformly distributed in the PDMS. In order to prepare PDMS/graphene composite with uniform resistance, a tetrahydrofuran solution is used to decrease the viscosity of a PDMS base polymer solution. A horn-type sonicator is then used to mix the base polymer with graphene flakes. Low viscosity of the base polymer solution improves the reliability and reproducibility of the PDMS/graphene composite for strain sensor applications. After dicing the composite into the desired sensor shape, a tensile test is performed. The experimental results show that the composite with a concentration of 30 wt.% exhibits a linear response up to a strain rate of 9%. The graphene concentration of the prepared materials affects the gauge factor, which at 20% graphene concentration reaches about 50, and with increasing graphene concentration to 30% decreases to 9. Furthermore, photolithography, PDMS casting, and a stencil process are used to fabricate a PDMS cantilever with an integrated strain sensor. The change in resistance of the integrated PDMS/graphene sensor is characterized with respect to the displacement of the cantilever of within 500 μm. The experimental results confirmed that the prepared PDMS/graphene based sensor has the potential for high-sensitive biosensor applications. *Published by AIP Publishing.* [http://dx.doi.org/10.1063/1.4962925]

I. INTRODUCTION

Recently, many efforts have been made to develop sensors of low cost, fast response, and high sensitivity.[1–3] In accordance with the research trend in biosensors, advancement in microfabrication technology has been playing a large role in facilitating the low-cost mass production of sensors. Biosensors are mainly employed to analyze the reactions of target substances with DNA, enzymes, antigens, antibodies, and biochemical substances, as well as to examine the biological/mechanical characteristics of cells.[4–11] Materials having biocompatibility, such as polydimethylsiloxane (PDMS) and SU-8 polymers, are mainly used in the microfabrication of biosensors, which sense information from a measurement target through various methods and convert it into useful signals that can be read by observers.[12,13] In previous reports, a fluorescent substance, surface plasmon resonance (SPR), and cantilever sensor were typically used to measure target signals in the biosensor.[14–16] In particular, optical measurement based on the fluorescence phenomena and SPR methods provides high-sensitivity measurement but requires a considerable amount of measurement time and expensive analysis equipment. An alternative is the cantilever sensor that employs a tiny piezoresistor on its surface.[1,2,17,18] The integrated sensor directly measures the change of physical properties induced by differential surface stress, mass changes, and the adsorption or attachment of analyte on the cantilever surface. Cantilever devices integrated with the piezoresistive sensor are widely used in the field of low-price sensors, as they can quickly provide the desired signal in real time.[3] Recently, various cantilever sensors have been studied to improve their sensitivity in biosensors.[19–21] The selection of cantilever material to enhance the sensitivity is one of the important issues. The cantilever used in the biosensor was commonly fabricated by silicon, SU-8, PDMS, or silicon dioxide (SiO_2).[22–26] Among the many materials, PDMS provides an advantage in sensitivity because in comparison with other materials, it has a lower Young's modulus. However, in comparison with doped silicon cantilevers, the PDMS cantilever sensitivity still need to be improved for wide applications. This is due to the lower gauge factor of the integrated piezoresistive sensor that is made by a thin metal film.

The piezoresistive sensor is a device in which when the sensor is subjected to strain, the resistance changes. Metals, doped silicon, and carbon composites can be employed as thin materials for fabricating strain sensors.[27–35] Conventional piezoresistive sensors in macro-systems employ metals with a simple fabrication process, such as aluminum; however, they have low sensitivity, with a gauge factor of 1–2. In microdevices, doped silicon is widely employed thanks to its excellent gauge factor (of 50 or even higher), but it requires an ion implantation process for the precise control of doping concentration and depth.[30,31] Recently, many studies have been actively conducted to obtain various composites with excellent gauge factor and simple fabrication process. The researches have focused on the use of carbon nanotubes, fullerene, silver nanowires, and graphene.[34,35]

[a]Y.-S. Choi and M.-J. Gwak contributed equally to this work.
[b]Author to whom correspondence should be addressed. Electronic mail: mems@jnu.ac.kr

In this study, the mechanical and electrical characteristics of a PDMS/graphene composite employed as a strain sensor were evaluated, and a PDMS cantilever integrated with the PDMS/graphene composite sensor was characterized for biosensor applications. The measured gauge factors of the PDMS/graphene composite sensors were in 9–50 range, depending on the graphene concentration in the composites. The reproducibility of the composite sensors was improved by using a horn-type sonicator and a diluted PDMS base solution to evenly distribute the graphene inside the composite. A simple photolithography process and a PDMS casting process were used to fabricate the sensor-integrated PDMS cantilever. The PDMS/graphene composite was used as a displacement measurement sensor to measure the displacement of the PDMS cantilever in real time. The fabricated PDMS cantilever can be used as a biosensor to detect cell force, enzymes, antigens, and antibodies.

II. DESIGN AND FABRICATION

A. Fabrication of PDMS/graphene composite

Figure 1(a) shows the fabrication process for the PDMS/graphene composite. High-purity graphene nanopowder (Graphene Supermarket) and Sylgard 184 PDMS (Dow Corning) were used. Among the various polymer materials, PDMS is an optically transparent, biologically suitable substance with excellent flexibility and an appropriate material for strain sensors.[30] To fabricate a reproducible PDMS/graphene composite, the viscosity of the PDMS base polymer must be reduced because the PDMS base polymer, which has high viscosity, needs to be evenly mixed with the graphene flakes. To accomplish this, as a first step in composite fabrication, the base polymer is added to a 20-ml tetrahydrofuran (THF) solution with good solubility, and the mixture is stirred for 2 h at 200 W power using a bath-type sonicator. This yields a liquid state with low viscosity. Simultaneously, to shorten the fabrication time, graphene is added to the THF solution and dispersed using a horn-type sonicator for 2 h at 200 W, until it is evenly mixed throughout the THF solution. The localized power of the horn-type sonicator provides higher intensity, compared to the bath-type. To evenly mix dispersed graphene in the THF solution and base polymer, the two prepared solutions are mixed in one container and dispersed using the horn-type sonicator for 8 h at 700 W and for 2 h at 280 W. By this time, most of the THF used as a solvent has evaporated because of the heat produced in the dispersion process involving the sonicator. After most of the THF has evaporated, the mixture of the base polymer and graphene is cooled at room temperature for 2 h. Then, a curing agent (Sylgard 184, Dow Corning) is added to the mixture of the graphene and base polymer in the ratio of 1:10, and the solution is mixed again using an ultrasonic generator. To remove residual THF and bubbles produced inside the mixed solution, it is placed inside a low-vacuum chamber for 30 min. The fabrication of the composite is completed by curing at 40 °C for 4 h and at 65 °C for 4 h, using a hotplate. The curing conditions are very important in determining the electrical characteristics of the composite. If the composite is rapidly cured using the hotplate at high temperature, residual THF in the composite evaporates rapidly, and this breaks electrical pathways between the graphene flakes, resulting in the problem of electrically disconnecting the composite. Therefore, when residual THF is gradually evaporated at low temperature, a composite having uniform electrical characteristics can be fabricated without any internal damage. Additionally, the composite preparation was conducted in both an ultrasonic bath and a horn-type sonicator, in order to reduce the production time and increase the efficiency. The bath-type ultrasonic method was employed for the step 1 sample (THF+PDMS). The horn-type ultrasonic method was employed for the step 2 sample (THF+Graphene), which mixed them very well because it could provide more concentrated energy than the bath-type method. The two processes were done in parallel to reduce the total time in sample preparation. Finally, we utilized the horn-type ultrasonic method to realize the step 3 sample (THF+PDMS+graphene). Figure 1(b) shows the time versus power level curves of the sonication process. Generally, when the bath-type is employed for step 2, more fabrication time is required.

B. Design and fabrication of the PDMS cantilever

PDMS with high biocompatibility was employed as the material of the cantilever intended for use as the biosensor. The dimensions of the PDMS cantilever were 9000 μm length, 3000 μm width, and 100 μm thickness. During the design stage of the PDMS cantilever, a spring constant value of about 1 nN/μm was employed because this value is appropriate for

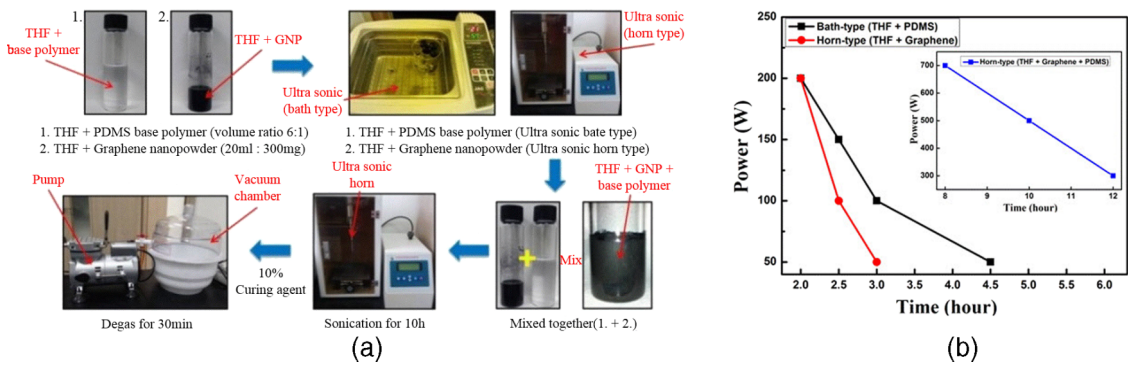

FIG. 1. (a) Sequence of the PDMS/graphene composite fabrication and (b) time versus sonication power level curves of the bath type and horn type sonication processes.

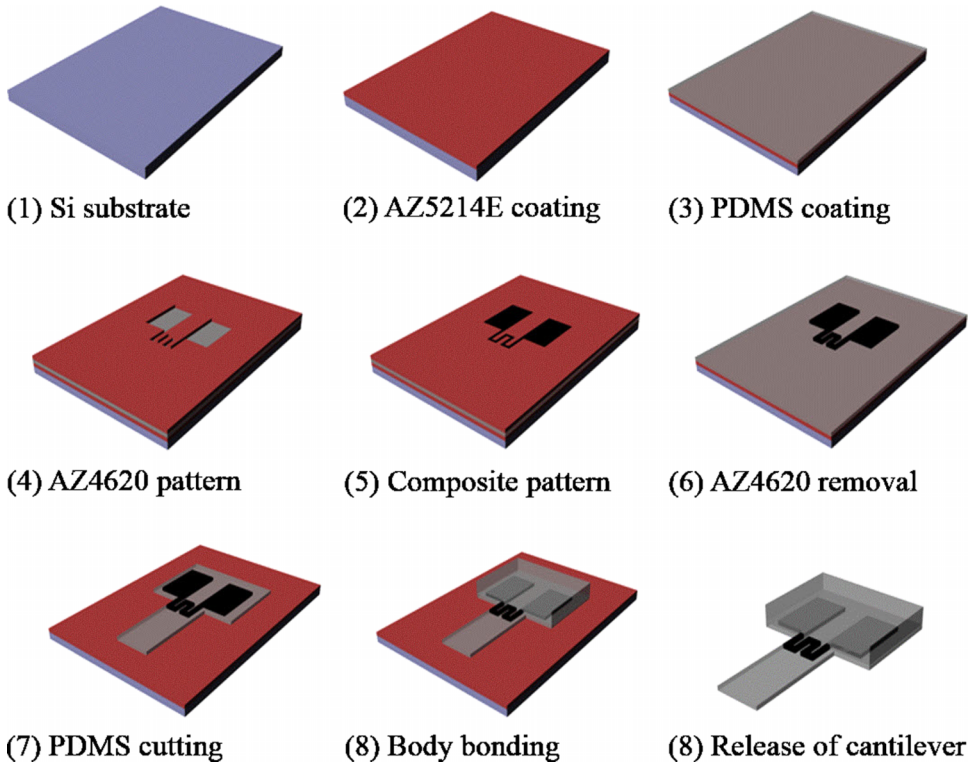

FIG. 2. A schematic diagram of the fabricating PDMS cantilever integrated with a PDMS/graphene composite piezoresistive sensor.

measuring the contraction force of cardiac muscle cells.[6,8,9] Conventionally, the piezoresistive sensors are placed on the cantilever as close as possible to its clamped edge or fixed end to achieve maximum stress during cantilever deflection, which allows the cantilever to have the highest sensitivity to force change (deflection change).

Figure 2 shows a schematic diagram of the process flow for the fabrication of the PDMS cantilever with composite sensor. An AZ5214 photoresist (PR) used as a sacrificial layer was spin-coated to a thickness of 2 μm on an n-type (100) silicon wafer (Fig. 2, (2)). This material increases the efficiency of fabrication by reducing the time needed to separate the cantilever device on the silicon wafer substrate, compared with a conventional Al sacrificial layer. The spin-coating time and speed determined the thickness of the PDMS layer formed on the PR (Fig. 2, (3)). The ratio of the base polymer to the curing agent used for the PDMS layer was 10:1. To form the PDMS/graphene composite sensor on the PDMS layer, a mold was fabricated by patterning the AZ4620 photoresist on the PDMS layer (Fig. 2, (4)). After O_2 plasma was used to make the PDMS surface hydrophilic, a photolithography process was performed to evenly coat PR on the PDMS surface. After filling the PDMS/graphene composite in the fabricated PR mold, the composite was cured for 4 h at 40 °C and for an additional 4 h at 65 °C on a hotplate (Fig. 2, (5)). After the composite was appropriately cured, the PR was removed with acetone, and the spin-coated PDMS layer was cut to the designed cantilever size using a blade (Fig. 2, (7)). The cantilever body was fabricated using an acryl mold obtained through CNC processing, and the fabricated PDMS body and PDMS cantilever surface were then joined through O_2 plasma treatment (Fig. 2, (8)). Finally, an AZ100 remover was used to remove the AZ5214 sacrificial layer to complete the fabrication of the PDMS cantilever (Fig. 2, (9)). Figure 3 shows optical images of the PDMS cantilever integrated with the PDMS/graphene composite sensor.

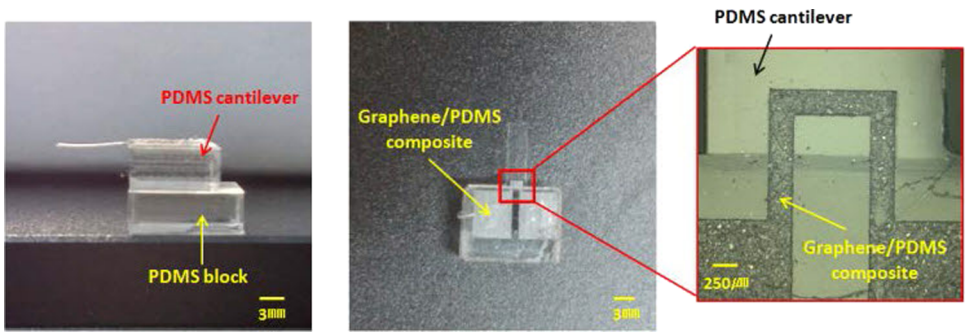

FIG. 3. Optical images of the PDMS cantilever integrated with PDMS/graphene composite sensor.

III. EXPERIMENTAL RESULTS AND DISCUSSION

A. Mechanical and electrical properties of PDMS/graphene composite

A universal tensile tester (Shimadzu, EX-SX) was used at room temperature to evaluate the mechanical properties of the fabricated PDMS/graphene composite according to the graphene concentration. The fabricated PDMS/graphene composite samples used in the tensile test were 22 (length) × 3 (width) × 0.5 (thickness) mm in size. In this work, we prepared different wt.% (15, 20, 25, and 30) of PDMS/graphene composite. However, the initial resistance of below 20% PDMS/graphene composite material was not stable. Therefore, to ensure reproducibility of the measurement results, five samples each were fabricated with three different graphene concentrations (20, 25, and 30 wt.%), and the average result of five repeated measurements was obtained. Figure 4(a) shows the strain-to-stress characteristics of the PDMS/graphene composite with respect to the graphene concentration. The Young's modulus measurement results for the 20, 25, and 30 wt.% samples were 1.27, 0.45, and 0.31 MPa, respectively; further, the Young's modulus of pure PDMS fabricated under the same curing conditions was 1.1 MPa. From these experiment results, it can be inferred that a low-concentration (≤20%) graphene composite has a larger Young's modulus than pure PDMS and that the Young's modulus of the composite, compared to pure PDMS cured under the same conditions, decreases at higher graphene concentrations (≥25%). This is because as the amount of graphene flakes inside the composite increases above a certain amount, the tensile strength of the composite decreases.[33]

The I–V characteristics measured by source meter (Keithley 2400) were used to calculate the electrical characteristics of the PDMS/graphene composite. The samples used for evaluating the electrical and mechanical characteristics of the composite were equal in size. These samples were also fabricated with three different graphene concentrations (20, 25, and 30 wt.%). During the measurement, electrical wires were connected using a conductive epoxy at both ends of the composite samples, and the current flowing within the voltage range of −0.3 to +0.3 V was measured. Figure 4(b) shows the conductivity with respect to the graphene concentration of the fabricated PDMS/graphene composite sensor. As indicated by the measurement results, increasing graphene concentration inside the composite decreased the electrical resistance, yielding a composite sensor with excellent reproducibility. When the graphene concentration was 30 wt.%, the resistance of the composite sample was 5.4 kΩ. The resistance error range was ±6% with excellent reproducibility; however, as the graphene concentration decreased, the resistance error range increased, even though the sensitivity was high. This was because the electrical network through the graphene flakes was imperfect at low graphene concentration. In this study, the PDMS/graphene composite sensor with a graphene concentration of 30 wt.% was used to fabricate the PDMS cantilever.

B. Electromechanical properties of the PDMS/graphene composite

To evaluate the electromechanical properties of the PDMS/graphene composite, changes in its resistance with mechanical strain were measured for various graphene concentrations. To apply tensile strain, a universal tensile tester (Shimadzu, EX-SX) was used to subject the samples to tensile force at room temperature at a rate of 0.5 mm/min (within 10%). The samples were identical in size to those used to evaluate the mechanical and electrical properties, and the relationship between the strain and change in resistance was measured for three different graphene concentrations (20, 25, and 30 wt.%). Figure 5(a) shows the relative changes in resistance with respect to the strain of the PDMS/graphene composites for three graphene concentrations. The test results indicate that as the graphene concentration decreases, the relative change in resistance for the strain of the PDMS/graphene composite increases. This is because the tunneling effect greatly influences the electrical resistance changes in the composite. In the PDMS/graphene composite with a graphene concentration of 30 wt.%, the relative change in resistance with strain is smaller than that in the other two samples; however because the relative change in resistance exhibits a linear characteristic up to 9% strain, this composite has an advantage in sensor applications.

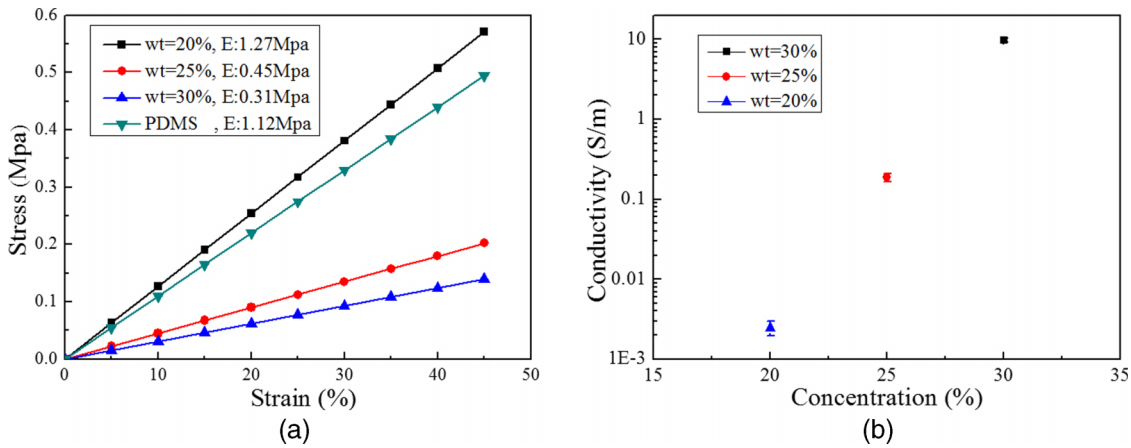

FIG. 4. (a) Mechanical characteristics of fabricated PDMS/graphene composite with respect to graphene concentration and (b) conductivity characteristics of composite with respect to graphene concentration.

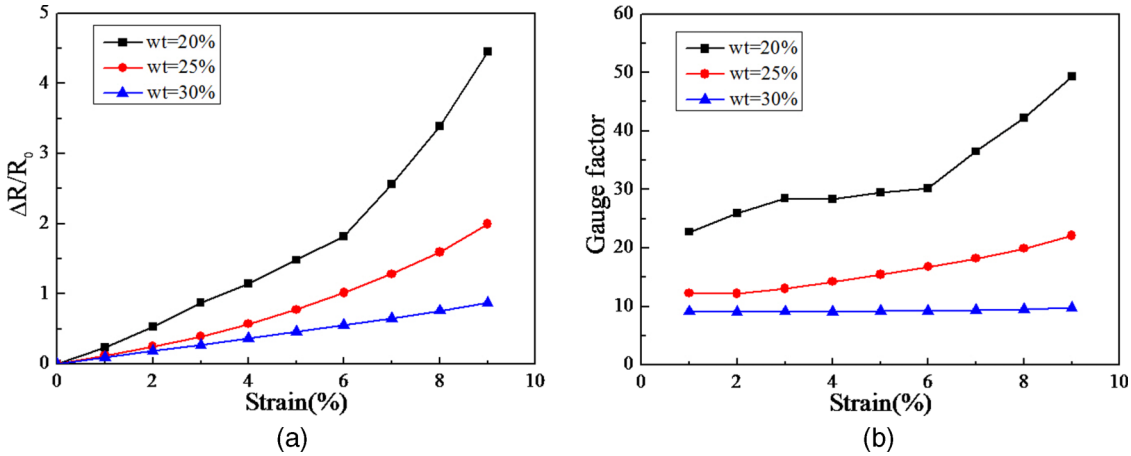

FIG. 5. (a) Relative changes in resistance of fabricated PDMS/graphene composite with respect to the strain for various graphene concentrations and (b) changes in the gauge factor of composite with respect to the strain for various graphene concentrations.

The electrical/mechanical sensitivity of the PDMS/graphene composite is determined by the gauge factor, which is the ratio of the resistance change ($\Delta R/R$) to the mechanical strain change ($\Delta L/L$) in the sample. Figure 5(b) shows changes in the gauge factor of the PDMS/graphene composite with respect to the strain for three graphene concentrations. According to the experimental results, when the graphene concentration is low and the strain increases, the gauge factor is excellent. However, for the samples with 20% and 25% concentrations, the gauge factor increases nonlinearly. As previously mentioned, nonlinear characteristics appear when a low amount of graphene flakes is added to the composite; this is because the tunneling effect mainly affects electrical resistance change with the mechanical strain in the sample. In contrast, the composite with a graphene concentration of 30 wt.% exhibits a gauge factor with linear output in a wide band, with higher sensitivity than that of the conventional metal strain gauge. To increase the sensitivity of the sensor, it is appropriate to use a PDMS/graphene composite having a low graphene concentration. However

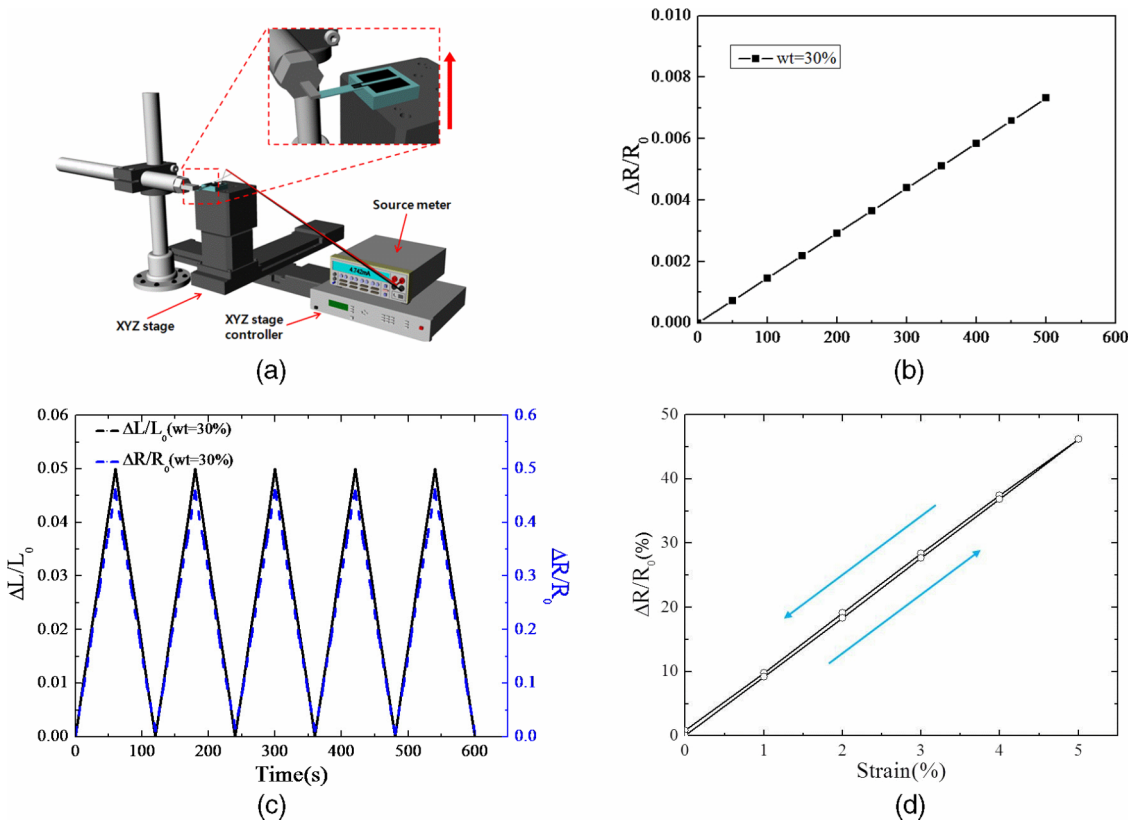

FIG. 6. (a) Schematic of a system to measure changes in resistance of the sensor with respect to cantilever displacement, (b) changes in resistance of the PDMS/graphene composite piezoresistive sensor having a graphene concentration of 30 wt.% with respect to displacement of the PDMS cantilever, (c) repeatability of the PDMS/graphene sensor under tensile stress, and (d) hysteresis characteristics of PDMS/graphene composite with graphene concentration of 30 wt.%.

because the electromechanical characteristics of the strain sensor have a nonlinear characteristic, it is necessary to select an appropriate graphene concentration for the given application. For example, although the sensitivity of a high-concentration PDMS/graphene composite sensor is lower than that of a low-concentration sensor, a high-concentration composite has better linear-response characteristics when it is used as a strain sensor in a narrow strain-change region. In this study, the displacements of the PDMS cantilever due to external force were characterized using the PDMS/graphene composite with a graphene concentration of 30 wt.%.

C. PDMS cantilever integrated with high-sensitive PDMS/graphene composite

To measure changes in the resistance of the composite sensor with respect to the displacement of the PDMS cantilever, a measurement system was designed and constructed that comprised a source meter (Keithley 2410), a motorized stage, a microscope, and LabVIEW. Figure 6(a) shows a conceptual diagram of the measurement system. Using the motorized stage on the PDMS cantilever integrated with the PDMS/graphene composite sensor, changes in the resistance of the sensor were measured with respect to the tensile stress acting on it, while displacement was applied at intervals of 50 μm. Figure 6(b) shows changes in the resistance of the sensor with respect to the displacement of the PDMS cantilever. When a displacement of ~500 μm was observed at the end of the cantilever, a resistance change of $\Delta R/R_0 = 0.008$ was observed. At this time, the gauge factor had a value of approximately 9, which was equal to the value obtained through basic experiment. The sensitivity of the PDMS/graphene composite sensor in this range was approximately four times that of a conventional commercial metal strain sensor (AGS-Tech, Inc., BF series) with a gauge factor of 2.2. At a cantilever displacement of 500 μm or higher, the change in resistance of the composite starts to exponentially increase. This nonlinear behavior in the gauge factor was dominant for the composite with lower graphene concentration. The fabricated PDMS/graphene composite with 30 wt.% has a linear characteristic within the strain range of 9% and nonlinear characteristic over a strain of 9%. Furthermore because the gauge factor rapidly increases, it is possible in the case of a cantilever operating under large tensile stress to implement a strain sensor with very high sensitivity. Figure 6(c) shows the repeatability of the PDMS/graphene strain sensor under tensile stress. Figure 6(d) shows the hysteresis characteristics of the PDMS/graphene composite with a concentration of 30 wt.%. The biocompatibility of the PDMS cantilever was also experimentally confirmed by measuring the contractility of cardiac muscle cells.[36–38] In the near future, the sensor-integrated PDMS cantilever will be applied to precisely measure the contraction force generated by cardiac muscle cells.

IV. CONCLUSIONS

In this study, a PDMS cantilever integrated with a PDMS/graphene composite sensor was fabricated for biosensor applications, and the mechanical and electrical properties of the sensor were evaluated using various equipments. The PDMS cantilever integrated with high-sensitivity sensor was fabricated by a simple photolithography process and a PDMS/graphene composite casting process. To obtain a PDMS/graphene composite sensor having uniform resistance, a horn-type sonicator and a diluted PDMS base solution were used to evenly disperse graphene inside the composite. As the graphene concentration increased, the electrical resistance of the fabricated PDMS/graphene composite decreased, yielding a composite sensor with excellent reproducibility. When the graphene concentration was 30 wt.%, the resistance of the PDMS/graphene composite sample was 5.4 kΩ and the resistance error was in the ±6% range, exhibiting excellent reproducibility. The fabricated PDMS/graphene composite showed piezoresistive characteristics and was used as a displacement measurement sensor by integrating it with a cantilever. Experimental results indicated that the relative change in resistance exhibits a linear characteristic up to 9% strain. Very high sensitivity was also achieved in the case of a large strain because as the displacement of the PDMS cantilever integrated with the PDMS/graphene composite sensor increases, the resistance change exponentially increases.

ACKNOWLEDGMENTS

This work was supported by the International Collaborative R&D Program through a KIAT grant funded by the MOTIE (Grant No. N0000894), the Korean Health Technology R&D project (Grant No. H113C1527) funded by the Ministry of Health & Welfare, and the National Research Foundation (NRF) Grant (No. 2015R1A4A1041746) by the Korea government.

[1]C. Ziegler, Anal. Bioanal. Chem. **379**, 946 (2004).
[2]L. G. Carrascosa, M. Moreno, M. Àlvarez, and L. M. Lechuga, TrAC, Trends Anal. Chem. **25**, 196 (2006).
[3]V. Seena, A. Rajorya, P. Pant, S. Mukherji, and V. R. Rao, Solid State Sci. **11**, 1606 (2009).
[4]J. Fritz, M. K. Baller, H. P. Lang, H. Rothuizen, P. Vettiger, E. Meyer, H.-J. Güntherodt, Ch. Gerber, and J. K. Gimzewski, Science **288**, 316 (2000).
[5]C. A. Savran, T. P. Burg, J. Fritz, and S. R. Manalis, Appl. Phys. Lett. **83**, 1659 (2003).
[6]X. R. Zhang and X. Xu, Appl. Phys. Lett. **85**, 2423 (2004).
[7]K. W. Wee, G. Y. Kang, J. B. Park, J. Y. Kang, D. S. Yoon, J. H. Park, and T. S. Kim, Biosens. Bioelectron. **20**, 1932 (2005).
[8]A. W. Feinberg, P. W. Alford, H. Jij, C. M. Ripplinger, A. A. Werdich, S. P. Sheehy, A. Grosberg, and K. K. Parker, Biomaterials **33**, 5732 (2012).
[9]A. Agarwal, J. A. Goss, A. Cho, M. L. McCain, and K. K. Parker, Lab Chip **13**, 3599 (2013).
[10]J. Kim, J. Park, K. Na, S. Yang, J. Baek, E. Yoon, S. Choi, S. Lee, K. Chun, J. Park, and S. Park, J. Biomech. **41**, 2396 (2008).
[11]M. L. Rodriguez, B. T. Graham, L. M. Pabon, S. J. Han, C. E. Murry, and N. J. Sniadecki, J. Biomech. Eng. **136**, 051005 (2014).
[12]M. Calleja, J. T. M. Nordström, and A. Boisen, Appl. Phys. Lett. **88**, 113901 (2006).
[13]Y. Zhao and X. Zhang, Sens. Actuators, A **136**, 491 (2007).
[14]S. K. Hartwell and K. Grudpan, Microchim. Acta **169**, 201 (2010).
[15]X. D. Hoa, A. G. Kirk, and M. Tabrizian, Biosens. Bioelectron. **23**, 151 (2007).
[16]S. Shin, J. P. Kim, S. J. Sim, and J. Lee, Appl. Phys. Lett. **93**, 102902 (2008).
[17]K. Zinoviev, C. Dominguez, J. A. Plaza, V. Cadarso, and L. M. Lechuga, Appl. Opt. **45**, 229 (2006).

[18]N. V. Lavrik, M. J. Sepaniak, and P. G. Datskos, Rev. Sci. Instrum. **75**, 2229 (2004).
[19]J. Thaysen, A. Boisen, O. Hansen, and S. Bouwstra, Sens. Actuators, A **83**, 47 (2000).
[20]P. A. Rasmussen, J. Thaysen, O. Hansen, S. C. Eriksen, and A. Boisen, Ultramicroscopy **97**, 371 (2003).
[21]P. A. Rasmussen, O. Hansen, and A. Boisen, Appl. Phys. Lett. **86**, 203502 (2005).
[22]M. Nordstrom, S. Keller, M. Lillenmose, A. Johansson, S. Dohn, D. Haefliger, G. Blagoi, M. Havsteen-Jakobsen, and A. Boisen, Sensors **8**, 1595 (2008).
[23]P. Li and X. Li, J. Micromech. Microeng. **16**, 2539 (2006).
[24]P. Li, X. Li, G. Zuo, J. Liu, Y. Wang, M. Liu, and D. Jin, Appl. Phys. Lett. **89**, 074104 (2006).
[25]Y. Chen, J. Li, P. Xu, M. Liu, and X. Li, in *Proceeding of 23rd IEEE International Conference on Micro Electro Mechanical Systems* (IEEE, 2010), pp. 859–862.
[26]R. Raiteri, M. Grattarola, H. J. Butt, and P. Skládal, Sens. Actuators, B **79**, 115 (2001).
[27]C. Stampfer, T. Helbling, D. Obergfell, B. Schoberle, M. K. Tripp, A. Jungen, S. Roth, V. M. Bright, and C. Hierold, Nano Lett. **6**, 233 (2006).
[28]J. Tong, M. Priebe, and Y. Sun, in *Proceeding of 20th IEEE International Conference on Micro Electro Mechanical Systems* (IEEE, 2007), pp. 843–846.
[29]C. K. M. Fung, M. Q. H. Zhang, R. H. M. Chan, and W. J. Li, in *Proceeding of 18th IEEE International Conference on Micro Electro Mechanical Systems* (IEEE, 2005), pp. 251–254.
[30]T. Toriyama and S. Sugiyama, J. Microelectromech. Syst. **11**, 598 (2002).
[31]C. Liu, *Foundations of MEMS* (Pearson Education Inc., NJ, 2006).
[32]K. Lee, S. S. Lee, J. A. Lee, K.-C. Lee, and S. Ji, Appl. Phys. Lett. **96**, 013511 (2010).
[33]P. Costa, J. Silva, A. Anson-Casaos, M. T. Martinez, M. J. Abad, J. Viana, and S. Lanceros-Mendez, Composites, Part B **61**, 136 (2014).
[34]B. Wang, B.-K. Lee, M.-J. Kwak, and D.-W. Lee, Rev. Sci. Instrum. **84**, 105005 (2013).
[35]C. Lee, L. Jug, and E. Meng, Appl. Phys. Lett. **102**, 183511 (2013).
[36]P. W. Alford, A. W. Feinberg, S. P. Sheehy, and K. K. Parker, Biomaterials **13**, 3613 (2010).
[37]J. You, H. Moon, B. Y. Lee, J. Y. Jin, Z. E. Chang, S. Y. Kim, J. Park, Y. S. Hwang, and J. Kim, J. Biomech. **47**, 400 (2014).
[38]K. Kim, R. Taylor, J. Y. Sin, S. J. Park, J. Norman, G. Fajardo, D. Bernstein, and B. L. Pruitt, Micro. Nano Lett. **6**, 317 (2011).